JACS
JOURNAL OF THE AMERICAN CHEMICAL SOCIETY
Article
pubs.acs.org/JACS

Precise Sequence Control in Linear and Cyclic Copolymers of 2,5-Bis(2-thienyl)pyrrole and Aniline by DNA-Programmed Assembly

Wen Chen and Gary B. Schuster*

School of Chemistry and Biochemistry, Georgia Institute of Technology, Atlanta, Georgia 30332, United States

Supporting Information

ABSTRACT: A series of linear and cyclic, sequence controlled, DNA-conjoined copolymers of aniline (ANi) and 2,5-bis(2-thienyl)pyrrole (SNS) were synthesized. In one approach, linear copolymers were prepared from complementary DNA oligomers containing covalently attached SNS and ANi monomers. Hybridization of the oligomers aligns the monomers in the major groove of the DNA. Treatment of the SNS- and ANi-containing duplexes with horseradish peroxidase (HRP) and H_2O_2 causes rapid and efficient polymerization. In this way, linear copolymers $(SNS)_4(ANi)_6$ and $(ANi)_2(SNS)_2(ANi)_2(SNS)_2(ANi)_2$ were prepared and analyzed. A second approach to the preparation of linear and cyclic copolymers of ANi and SNS employed a DNA encoded module strategy. In this approach, single-stranded DNA oligomers composed of a central region containing $(SNS)_6$ or $(ANi)_5$ covalently attached monomer blocks and flanking 5′- and 3′-single-strand DNA recognition sequences were combined in buffer solution. Self-assembly of these oligomers by Watson−Crick base pairing of the recognition sequences creates linear or cyclic arrays of SNS and ANi monomer blocks. Treatment of these arrays with HRP/H_2O_2 causes rapid and efficient polymerization to form copolymers having patterns such as cyclic BBA and linear ABA, where B stands for an $(SNS)_6$ block and A stands for an $(ANi)_5$ block. These DNA-conjoined copolymers were characterized by melting temperature analysis, circular dichroism spectroscopy, native and denaturing polyacrylamide gel electrophoresis, and UV−visible−near-IR optical spectroscopy. The optical spectra of these copolymers are typical of those of conducting polymers and are uniquely dependent on the specific order of monomers in the copolymer.

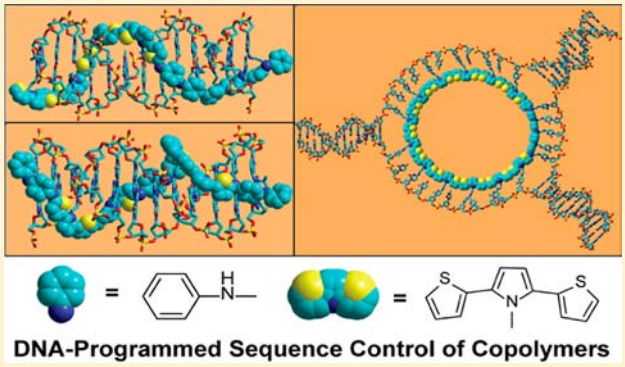

INTRODUCTION

Nucleic acids and proteins are biopolymers whose specifically ordered sequences of connected monomers confer distinct properties. The unique nucleotide sequence of a gene or the amino acid sequence of a protein creates complexity and assures the structural and functional diversity required for living organisms. Inspired by the biological process for producing specifically ordered polymers, scientists are striving to construct synthetic polymers with controlled sequences of monomers,[1−13] including the use of approaches that mimic natural assembly.[8−13] For example, DNA (or a polyelectrolyte such as polystyrene sulfonate) has been used as a scaffold for the enzymatic formation of conducting polymers under mild condition by which monomers are adsorbed and aligned through ionic interactions. The scaffold provides a local environment that facilitates polymerization and controls the structure of the polymer.[14−21] However, this method yields only homopolymers that do not incorporate information from the nucleobase sequence. We recently developed a DNA-directed synthetic approach that enables the formation of information-rich conducting polymers.[22−27] In this method, the monomers of conducting polymers (e.g., aniline; ANi) are preorganized by covalent linkage to a nucleobase. Self-assembly aligns the monomers in the DNA major groove thus facilitating the programmed construction of specific conducting polymers by their reaction with horseradish peroxidase (HRP) and H_2O_2. The sequence programmability of this approach was demonstrated by using aniline and benzene monomers linked to alternating cytosines on DNA oligomers in the synthesis of copolymers.[23] More recently, we reported the use of a modular DNA assembly strategy for the programmed polymerization of 2,5-bis(2-thienyl)-pyrrole (SNS) monomers into a variety of linear and closed-cycle arrays of conducting polymers.[27] In this article, we report the extension of these DNA-directed synthetic methods to the preparation of copolymers of SNS and ANi with preprogrammed sequences and precisely controlled molecular architectures.

We employ two strategies to assemble and control the sequences of SNS and ANi monomers on DNA templates. In the "duplex" strategy, shown in Scheme 1, duplex DNA is assembled by hybridization of complementary single strands one of which is modified by covalent attachment of SNS monomers, represented by red spheres, (DNA(1) and

Received: December 21, 2012
Published: February 28, 2013

dx.doi.org/10.1021/ja312507z | J. Am. Chem. Soc. 2013, 135, 4438−4449

Scheme 1. Illustration of the "Duplex" Strategy for DNA-Templated Alignment of SNS and ANi Monomers in the DNA Major Groove and the Formation of Block and Interdigitated Copolymers[a]

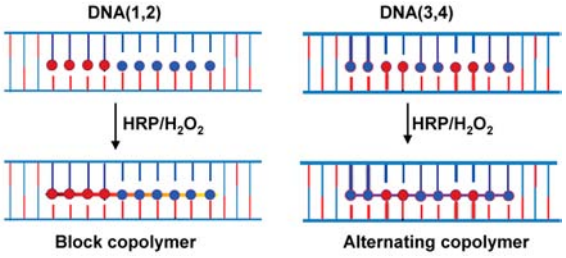

[a]The horizontal lines represent the DNA backbone, the vertical lines represent the DNA bases, the red spheres represent covalently attached SNS monomers, and the blue spheres represent ANi monomers. The actual DNA sequences are shown in Figure 1.

DNA(3), see Figure 1) and the other by attachment of ANi monomers, represented by blue spheres, (DNA(2) and DNA(4)). As depicted in Scheme 1, these duplex oligomers create unique sequences of assembled SNS and ANi monomers. The reaction of duplex DNA(1,2) with HRP/H_2O_2 is expected to generate the DNA-conjoined block copolymer $(SNS)_4(ANi)_6$. Similarly for DNA(3,4), there are four SNS monomers on one DNA strand and six ANi monomers on another arranged so that hybridization of the two complementary single strands creates a duplex with three interdigitated $(SNS)_2$ and $(ANi)_2$ steps. The reaction of duplex DNA(3,4) with HRP/H_2O_2 is expected to generate the DNA-conjoined copolymer $(ANi)_2(SNS)_2(ANi)_2(SNS)_2(ANi)_2$.

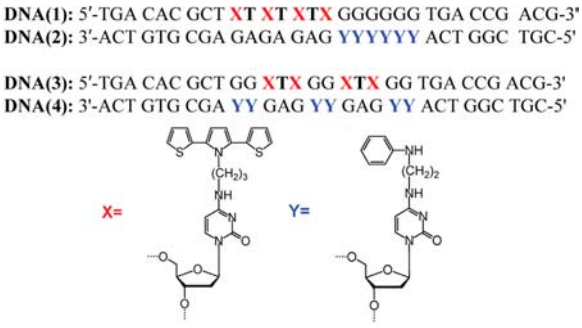

Figure 1. Structures of the SNS- and ANi- containing duplex oligomers.

In the "encoded modules" strategy, shown in Scheme 2, we prepare single-strand DNA oligomers ("modules", see Figure 5) composed of a central region containing covalently linked monomer units (SNS or ANi) and "recognition" sequences flanking the central region on its 5′- and 3′-sides. The recognition sequence of one module is coded to uniquely self-assemble by Watson–Crick pairing into a duplex with another module. This enables the spontaneous formation of the cyclic array (b1,b2,a3), see Figure 5, having ordered blocks of SNS and ANi monomers. Alternatively, the monomers may be assembled into the linear array (b1,a2,b4), see Figure 5, in which the "dangling" single-strand recognition sequences of the terminal modules are "capped" by complementary single-strand oligomers (caps, see Figure 5). Treatment of these cyclic or linear arrays of monomers with HRP/H_2O_2 is expected to generate the corresponding DNA-conjoined block copolymers with unique sequences determined by assembly of the DNA modules. The copolymers prepared by these DNA-templated, self-assembly strategies have precisely programmed sequences and well-defined structures. Their unique and readily controllable properties may enable their application as molecular wires in novel microelectronic devices and nanosensors.

METHODS

Instrumentation. UV–visible absorption (UV–vis) spectra were recorded on a Cary 1E spectrophotometer; UV melting and cooling curves were recorded using a multicell block and temperature

Scheme 2. Illustration of the "Encoded Modules" Strategy for DNA-Templated Alignment of SNS and ANi Monomers in Cyclic and Linear Arrays[a]

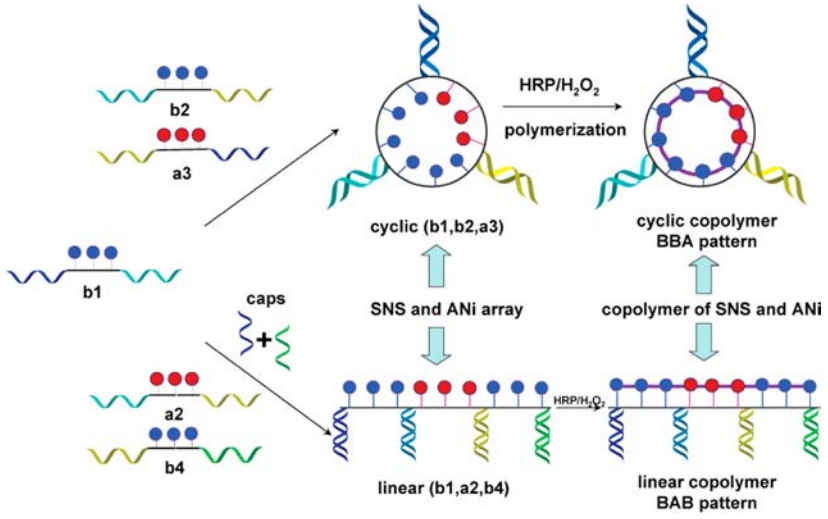

[a]The single-strand DNA recognition sequences are shown as color-coded wavy lines that indicate their affinity with complementary modules and ability to form duplex segments by Watson–Crick recognition. Red and blue spheres represent SNS and ANi monomers, respectively. B represents an $(ANi)_5$ block and A represents an $(SNS)_6$ block. The actual DNA sequences are shown in Figure 5.

dx.doi.org/10.1021/ja312507z | J. Am. Chem. Soc. 2013, 135, 4438–4449

controller on the spectrophotometer. UV−vis−near-IR (UV−vis−NIR) spectra were recorded on a Cary 5E spectrophotometer. Circular dichroism (CD) spectra were recorded on a JASCO J-715 spectropolarimeter. Electrospray ionization mass spectrometry (ESI-MS) spectra were recorded on an Applied Biosystems QSTAR-XL in negative ion mode.

Materials. All reagents were used as received without further purification. SNS with a *N*-propylamine linker was prepared by the previously reported method.[26] *N*-Phenylethylenediamine was purchase from Sigma−Aldrich, St. Louis, MO. T4 polynucleotide kinase (PNK) enzyme was purchased from New England Biolabs Inc. γ-^{32}P-ATP was purchased from MP Biomedicals. HRP, type II (200 units/mg) and 2,2′-azino-bis(3-ethylbenzothiazoline-6-sulfonic acid) (ABTS) were purchased from Sigma−Aldrich. A stock solution of HRP was prepared by dissolving 2 mg of HRP in 1 mL of nanopure water. Hydrogen peroxide was purchased from Fischer Scientific, Pittsburgh, PA, and was diluted with nanopure water to 0.03% before use.

Preparation of Modified DNA Oligomers. The SNS- and ANi-containing DNA oligomers were synthesized and purified following previously developed methods.[25−27] The purified DNA oligomers were desalted using Waters Sep Pak cartridges and characterized by ESI-MS (see the Supporting Information). The concentrations of the modified DNA oligomers were determined by their absorption intensity at 260 nm with every two SNS or ANi groups counted as a cytosine.

Preparation of Radiolabeled DNA. The oligonucleotides were labeled at the 5′-terminus with γ-^{32}P-ATP and T4 kinase. The radiolabeled DNA samples were purified by 20% polyacrylamide gel electrophoresis (PAGE). The desired bands were excised from the gel and extracted with water at 37 °C for 12 h. The DNA was precipitated from the supernatant by addition of 0.03 M sodium acetate pH 5.2 and cold ethanol (800 μL for 300 μL of the supernatant). The mixture was vortexed, held at −78 °C for 60 min, and centrifuged for 60 min at 13 000 rpm. The supernatant was removed, and the residual DNA was washed two times with 100 μL of 80% ethanol and dried in a Speed Vac at medium heat. Suitable volumes of water were added for further experimentation.

Self-Assembly of SNS−DNA and ANi−DNA oligomers. Samples were prepared by mixing one equiv of each single-stranded DNA oligomer in 10 mM citrate buffer (pH 4.5) containing 200 mM NaCl. Capping DNA oligomers (2 equiv) were added to each modular linear assembly. Hybridization was achieved by heating the samples at 80 °C for 10 min and then slowly cooling in the dark to room temperature overnight. These samples were used for melting temperature (T_m) measurement, CD spectroscopy, and reaction with HRP/H_2O_2.

Copolymerization with HRP/H_2O_2. The reaction with HRP/H_2O_2 was carried out at room temperature in 1 mL of solution by the addition of 2 μL of HRP (2 mg dissolved in 1 mL of nanopure water) followed by 2−10 μL of H_2O_2 (0.03%) and 10 μL of ABTS (10 μM in water). UV−vis−NIR spectra were recorded before and after initiation of the reaction. For all of the reactions studied, the new absorption bands arising from the copolymerization reach maximum intensity within 10 min. After reaction with HRP/H_2O_2, 4 mM hydrazine was added to reduce the oxidized polymers to their leuco form.

T_m Measurements. Samples for T_m measurement before reaction with HRP/H_2O_2 were prepared by hybridizing 2 μM DNA strands in 10 mM sodium citrate buffer (pH 4.5) containing 200 mM NaCl. The thermal melting profiles were recorded with a heating and cooling rate of 1 °C/min. The change of absorbance at 260 nm was monitored to obtain the melting curve of the DNA oligomers. After reaction with HRP/H_2O_2, the T_m was measured in the same way. To obtain the melting curve of the SNS-containing arrays, the concentration of DNA was increased to 4 μM, and the change of absorbance during heating and cooling was monitored at 320 nm.

Nondenaturing PAGE Analysis. Nondenaturing gel experiments were performed to study the formation of the linear and cyclic assembly from the SNS−DNA and ANi−DNA oligomers. Samples for the gel experiments were prepared by mixing unlabeled (1 μM) and radiolabeled (6000 cpm) DNA oligomers in 10 mM sodium phosphate (pH 7.0) buffer containing 200 mM NaCl (total volume 100 μL). The samples were electrophoresed on a 10−14% 19:1 polyacrylamide gel in a Hoefer vertical slab gel unit model SE400 (Hoefer Scientific Instruments, San Francisco, CA). The bands on the wet gel were visualized by autoradiography.

Denaturing PAGE Analysis. Denaturing gel experiments were performed to study the linking of DNA oligomers due to the formation of linear or cyclic copolymers of SNS and ANi. Samples for the gel experiments were prepared by mixing unlabeled (1 μM) and radiolabeled (6000 cpm) DNA oligomers in 10 mM citrate buffer (pH 4.5) containing 200 mM NaCl (total volume 100 μL). The reaction with HRP/H_2O_2/ABTS was carried out at 5 °C for 30 min. Then, the pH was increased to 8 by adding 1 M NaOH, and this solution was mixed with 50 μL of denaturing loading buffer (formamide and water in 4:1 ratio). The samples were electrophoresed on a 7−10% 19:1 polyacrylamide gel containing urea (2.8−4 M) at 45 °C and visualized by autoradiography.

RESULTS

Duplex Strategy: DNA Cross-Linking by Templated Polymerization. We synthesized, purified, and characterized a series of DNA oligomers (see Figure 1) having covalently bound SNS and ANi groups according to previously described procedures[25−27] (see the Supporting Information, Table S1). DNA(1) and DNA(3) each have four covalently attached SNS monomers. In DNA(1), the SNS monomers are separated by a thymine so that the 5- and 5′-carbon atoms of adjacent SNS groups are within bonding distance. Similarly for DNA(3), two pairs of SNS monomers are separated by a thymine. DNA(2) and DNA(4) each have six covalently attached ANi monomers. In DNA(2), the six ANi monomers are linked to adjacent cytosines, which aligns them within bonding distance. In DNA(4), three pairs of ANi monomers are attached to adjacent positions. DNA(1) and DNA(2) are complementary as are DNA(3) and DNA(4). The hybridization of these complementary single strands is expected to form duplex oligomers in which both the SNS and ANi monomers are aligned in the major groove of the DNA. In duplex DNA(1,2), the SNS and ANi monomers are arrayed in a side-by-side pattern with four SNS monomers adjacent to six ANi monomers. In contrast, for duplex DNA(3,4), the SNS and ANi monomers are organized into a zipperlike array in which pairs of ANi monomers are separated by pairs of SNS monomers.

Characterization of SNS and ANi Arrays. The formation, stability, and structures of duplexes DNA(1,2) and DNA(3,4) were assessed by T_m measurements and by CD spectroscopy. The melting curves for DNA(1,2) and DNA(3,4) monitored at 260 nm in 10 mM sodium citrate buffer solution at pH 4.5 containing 200 mM NaCl show single transitions at 56.6 and 62.5 °C, respectively, and hyperchromicity of approximately 0.15 absorbance units (see the Supporting Information, Figure S1). Measurement of the T_m for DNA(3,4) monitored at 320 nm (where the absorption of SNS dominates) reveals a cooperative transition associated with unstacking of the SNS and ANi monomers (see the Supporting Information, Figure S2). The T_m observed at 320 nm is the same as that observed at 260 nm, indicating that the stability of the ordered SNS−ANi zipper array is governed by hybridization of the DNA duplex.[28,29] These observations show that these SNS- and ANi-linked oligomers form stable duplexes under the condition required for polymerization of the monomers initiated by reaction with HRP/H_2O_2.

CD spectroscopy was employed to study the conformations of the SNS- and ANi-modified DNA duplexes. Figure 2a and b

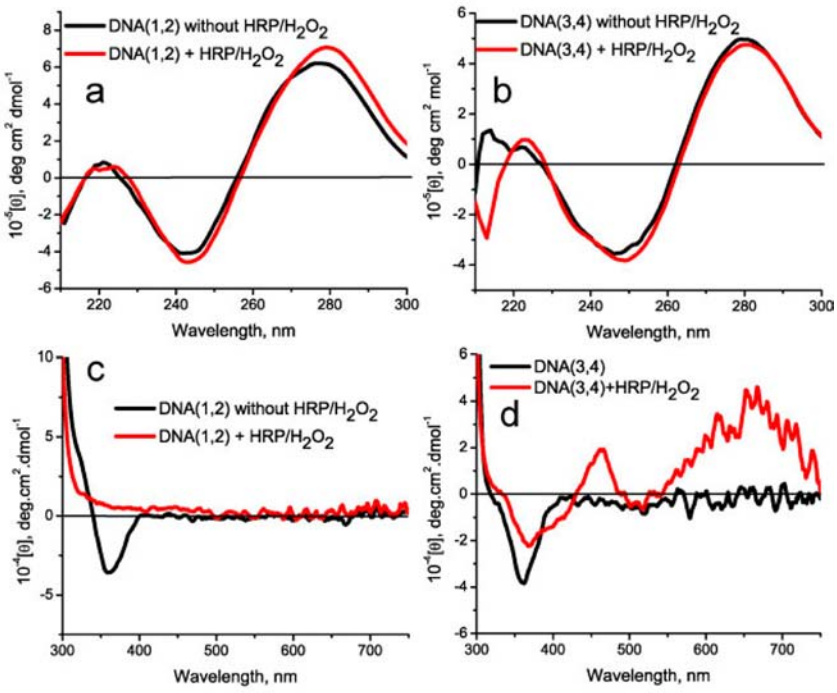

Figure 2. CD spectra of DNA(1,2) and DNA(3,4) before and after the reaction with HRP/H_2O_2. (a, b) 200−300 nm, DNA = 4 μM; (c, d) 300−750 nm, DNA = 20 μM.

shows the CD spectra of DNA(1,2) and DNA(3,4), respectively. Both DNA(1,2) and DNA(3,4) have a negative peak at approximately 245 nm and a positive peak at approximately 280 nm that are typical CD features of B-form DNA. Apparently, the SNS and ANi modifications do not significantly change the overall B-form helical conformation of the duplex DNA. At high concentration, the CD spectra (Figure 2c,d) of duplexes DNA(1,2) and DNA(3,4) show a weaker, negative band with a maxima at approximately 360 nm corresponding to the absorption of the SNS monomers. This induced CD band (ICD) is similar to that previously reported for DNA duplexes formed by hybridization of two complementary DNA single strands both having covalently linked SNS monomers in a zipperlike array.[29] The negative ICD band suggests that the SNS monomers form an ordered array with chirality induced by the right-handed helix of the DNA. The absorption of the ANi monomers overlaps that of the DNA bases thus obscuring a possible ICD band for this chromophore. However, previous molecular modeling studies have shown that the covalently linked ANi monomers are aligned in the major groove of the DNA.[23,25] Deconvolution of the UV absorption spectra for DNA(1,2) and DNA(3,4) reveals SNS absorption bands with a peaks at approximately 342 nm (the absorption maximum for a single SNS monomer linked to DNA is 348 nm), which is consistent with an H-aggregate-like structure for the SNS monomer array (see the Supporting Information, Figure S3).[30,31]

Sequence-Controlled Copolymers of SNS and ANi. We previously reported that DNA-conjoined ANi and SNS polymers are formed efficiently by the reaction of HRP/H_2O_2 and a catalytic amount of ABTS[32,33] with oligomers containing covalently attached monomers.[22,23,25−27] In the previous studies, each DNA oligomer contained only one type of monomer (SNS or ANi), and thus, homopolymers are formed. DNA(1,2) and DNA(3,4) are ordered arrays composed of both SNS and ANi monomers. Polymerization of the monomers in these double-strand oligomers is expected to generate copolymers and concomitantly covalently cross-link the duplexes. The reactions of these DNA oligomers with HRP/H_2O_2 were monitored by melting temperature, by denaturing PAGE to assess whether cross-linking of the two DNA strands had occurred, by UV−vis−NIR spectroscopy to reveal the optical absorption spectra of the copolymers in their leuco and polaron or bipolaron oxidation states, and by CD spectroscopy.

The reaction of DNA(1,2) and DNA(3,4) with HRP/H_2O_2 will covalently cross-link the duplexes, which is expected to make them more thermally stable and to retard their migration on a denaturing gel. The T_m values of DNA(1,2) and DNA(3,4) after reaction are 71 and 75 °C, respectively, which correspond to an increase of more than 10 °C compared with that of the unreacted duplexes. There is also a significant decrease in hyperchromicity on melting after the reaction with HRP/H_2O_2 that also suggests cross-linking of the oligomers (see the Supporting Information, Figure S1).

The products from reaction of DNA(1,2) and (3,4) with HRP/H_2O_2 were analyzed by denaturing PAGE; the results are shown in Figure 3. In this experiment, normal duplex DNA is denatured and migrates as single strands. Lanes 1 and 3 show the position on the gel of DNA(1*) and DNA(3*) radiolabeled with ^{32}P (indicated by the asterisk) at their 5′-ends for visualization by autoradiography. Lanes 2 and 4 show the results of the reactions of DNA(1*,2) and (3*,4) with HRP/H_2O_2, respectively. In both cases, the bands are strongly retarded and well separated from those of single strands DNA(1) and DNA(3). This finding shows that reaction results in the bond formation between SNS and ANi monomers that cross-links DNA(1,2) and DNA(3,4). Previous examination of the formation of conducting polymers from DNA-linked monomers shows that the absorption maxima of the polymers increase as expected with the number of monomers suggesting

dx.doi.org/10.1021/ja312507z | J. Am. Chem. Soc. 2013, 135, 4438−4449

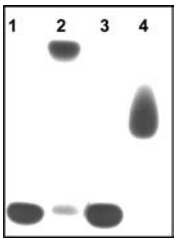

Figure 3. Denaturing PAGE analysis of DNA (1,2) and (3,4) after the reaction with HRP/H_2O_2. Lanes 1 and 3, ^{32}P-labeled DNA(1*) and DNA(3*); lane 2, DNA(1*,2) + HRP/H_2O_2; lane 4, DNA(3*,4) + HRP/H_2O_2.

that each monomer is incorporated in the polymer.[27,29] Furthermore, preorganization of monomers on a DNA scaffold has been shown to facilitate complete bonding even when the monomers are not adjacent.[34] In the present case, additional evidence for complete bond formation between the monomers comes from observation of a single melting transition after reaction with HRP/H_2O_2 and especially the essentially complete cross-linking of DNA(1) and DNA(2), lane 2 of Figure 2, which can only result from bond formation between the ANi and SNS monomers. Interestingly, DNA(3,4), which has four SNS–ANi cross-links and is thus more rigid than DNA(1,2), which has only one SNS–ANi cross-link, migrates considerably faster on the gel.

Conducting polymers have characteristic electronic absorption spectra. Figure 4a shows the UV–vis–NIR spectra from the reaction of DNA(1,2) with HRP/H_2O_2. There is a rapid decrease of the absorption of the SNS monomers at 340 nm upon mixing of the reagents accompanied by the appearance of new absorption bands with apparent maxima at approximately 420, 450, 660, and 950 nm. For comparison, under these conditions, the absorption spectrum of the homopolymer $(ANi)_6$ exhibits maxima at approximately 420 and 740 nm and that of $(SNS)_4$ has absorption peaks at approximately 416, 583, and 950 nm.[17,19−21] Thus, the weak 450 and the prominent 660 nm absorption bands observed from the reaction of DNA(1,2) with HRP/H_2O_2 are unique and indicate the formation of the copolymer $(SNS)_4(ANi)_6$. The 660 nm absorption band is also prominent in the spectrum from the reaction of DNA(3,4), Figure 4b, suggesting that the zipper array of SNS and ANi monomers is converted to the alternating copolymer with the sequence $(ANi)_2(SNS)_2(ANi)_2(SNS)_2(ANi)_2$. The reaction of these copolymers with hydrazine causes their reduction to the leuco oxidation state whose absorption spectra show shoulders at approximately 400 nm (see the Supporting Information, Figure S4).

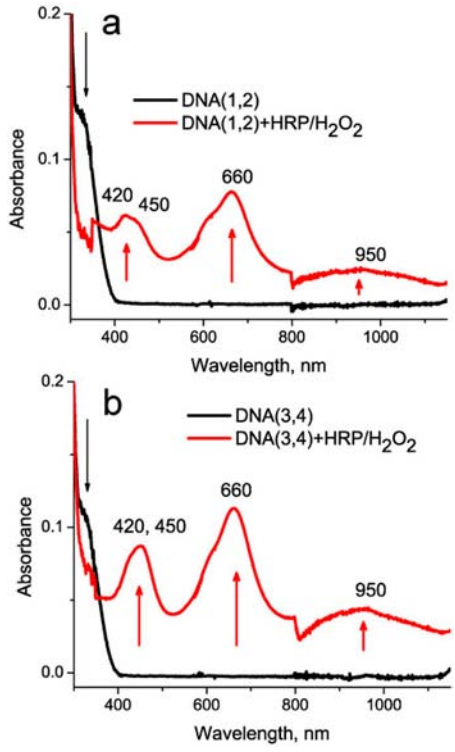

Figure 4. UV–vis–NIR spectra of (a) DNA(1,2) and (b) DNA(3,4) before and after the reaction with HRP/H_2O_2. The "glitch" at 800 nm is an instrumental artifact caused by switching to the NIR region.

The cross-linked copolymers were also analyzed by CD spectroscopy. The spectra of DNA(1,2) and DNA(3,4), shown in Figure 2a and b, indicate that the global structure of the DNA stays B-form like after reaction with HRP/H_2O_2. Figure 2d shows the CD spectrum in the visible region for a concentrated sample of DNA(3,4) after reaction with HRP/H_2O_2. The ICD band for the SNS monomer disappears, and two new positive CD peaks appear at approximately 460 and 660 nm, corresponding to the absorption of the oxidized SNS–ANi copolymer. These new ICD features indicate a linearly helical conformation of the copolymer that twists along with the major groove of the DNA duplex. The CD spectrum of DNA(1,2) after the reaction of HRP/H_2O_2 (Figure 2c) shows the loss of the ICD band for the SNS monomer but does not show an ICD for the copolymer.

Encoded Module Strategy: DNA-Programmed Assembly for Cyclic and Linear SNS and ANi Copolymers. We have previously shown that cyclic and linear arrays of SNS monomers can be formed by the programmed self-assembly of single-stranded DNA modules modified to contain covalently attached SNS monomers. These SNS monomers are readily converted to polymers by reaction with HRP/H_2O_2.[27] In this work, we demonstrate that this modular strategy can be used to assemble cyclic and linear SNS and ANi arrays for the synthesis of block copolymers having designed sequences. The SNS and ANi monomers are linked to central regions of individual single-strand DNA oligomers and then assembled through the formation of Watson–Crick base pairs by uniquely encoded flanking recognition sequences, see Scheme 2.

Characterization of Cyclic and Linear Arrays of SNS and ANi Monomers. The series of SNS- and ANi-containing DNA modules shown in Figure 5 were prepared, purified, and characterized by previously described methods (see the Supporting Information, Table S1). Modules a1–a6 each have six SNS monomers covalently bound to cytosines separated by a thymine in the central segment of the oligomers, shown as $(XT)_5X$, between uniquely coded flanking recognition sequences. DNA oligomers b1–b4 have the same recognition sequences as modules a1–a4, but in these cases, five ANi monomers covalently bound to cytosines $(Y)_5$ form the central segment. The 12-nucleotide recognition sequences on the 5′- and 3′-sides of the X- or Y-containing central segments enable unique self-assembly with modules containing complementary sequences.

As demonstrated previously, a cyclic array of SNS monomers is formed by assembly of modules (a1,a2,a3) into a closed structure having three DNA duplex "arms".[27] Because of

dx.doi.org/10.1021/ja312507z | J. Am. Chem. Soc. 2013, 135, 4438–4449

a1: 5′-AGC GCT TGG AGT $(XT)_5$X TGA GGT TCG CGA-3′
a2: 5′-TCG CGA ACC TCA $(XT)_5$X AGT GTG CTA CGT-3′
a3: 5′-ACG TAG CAC ACT $(XT)_5$X ACT CCA AGC GCT-3′
a4: 5′-ACG TAG CAC ACT $(XT)_5$X AAT GCC TCG AAG-3′
a5: 5′-CTT CGA GGC ATT $(XT)_5$X ACT CCA AGC GCT-3′
a6: 5′-CTT CGA GGC ATT $(XT)_5$X TGC ATA GCA ATG-3′
b1: 5′-AGC GCT TGG AGT $(Y)_5$ TGA GGT TCG CGA-3′
b2: 5′-TCG CGA ACC TCA $(Y)_5$ AGT GTG CTA CGT-3′
b3: 5′-ACG TAG CAC ACT $(Y)_5$ ACT CCA AGC GCT-3′
b4: 5′-ACG TAG CAC ACT $(Y)_5$ AAT GCC TCG AAG-3′
c1: 5′-ACT CCA AGC GCT-3′
c2: 5′-CTT CGA GGC ATT-3′
c3: 5′-TGA GGT TCG CGA-3′
c4: 5′-ACG TAG CAC ACT-3′

Figure 5. SNS- and ANi-linked DNA modules used for cyclic and linear assemblies. The color-coding represents Watson−Crick complementarity; for example, the blue recognition sequence starting at its 5′-end of a1 is complementary to the blue recognition sequence of a3 terminating at its 3′-end. X and Y have the same meaning as in Figure 1.

designed sequence similarity, when appropriate ANi-linked DNA modules are mixed with corresponding SNS-linked modules, the self-assembly process forms an array having a specific structure and a specific monomer order. For example, the hybridization of modules (b1,b2,a3) is expected to form a cyclic, three-armed array containing 10 ANi monomers and 6 SNS monomers, see Scheme 2. We refer to this arrangement of monomers as having a "cyclic BBA" pattern where B stands for an $(ANi)_5$ block and A stands for an $(SNS)_6$ block. Similarly, assembly of modules (b1,a2,a3) will form a cyclic array composed of 12 SNS monomers and 5 ANi monomers arranged in a cyclic BAA pattern. The encoded modules may also be used to assemble linear arrays of monomers. For example, modules (b1,a2,b4) are expected to form a linear array composed of 10 ANi monomers and 6 SNS monomers in a linear BAB pattern, see Scheme 2. In this case, the terminal recognition sequences are "capped" by duplex formation with the complementary DNA oligomers c1 and c2, see Figure 5.

The assembly of the DNA modules into cyclic and linear structures was assessed by monitoring melting temperatures and by nondenaturing PAGE. The cyclic assemblies show single melting transitions with observed T_m values in the range from approximately 61 °C for (b1,a2,b3), which has a BAB pattern, to approximately 70 °C for (a1,b2,a3) with a ABA pattern, see Figure 6a. The T_m values of the capped linear assemblies are consistently less than their cyclic counterparts with T_m values ranging from approximately 50 °C for (b1,b2,a4) to approximately 54 °C for (a1,b2,a4), see the Supporting Information, Figure S5 and Table S2. Apparently there is cooperative behavior in the cyclic assemblies that provides additional stabilization;[27,34] however, all assemblies are stable at room temperature under the conditions required for their reaction with HRP/H_2O_2.

Nondenaturing (native) PAGE, where duplexes migrate as intact double strands, was used to assess assembly of modules into linear and cyclic arrays. We labeled modules b1 and b2 with ^{32}P at their 5′-ends to enable their visualization by autoradiography. Figure 7 shows the native gels for the linear and cyclic structures. The single band in lane 1 shows the position of module b2*. Lanes 2 and 3 show that the linear dimers (a1, b2*) and (b1,b2*) remain intact under these conditions and migrate, as expected, more slowly than the single module. The cyclic assembly (a1,b2*,a3) shown in lane 4 and the linear assembly (a1,b2*,a4) shown in lane 5 both migrate more slowly than the linear dimers. The additional

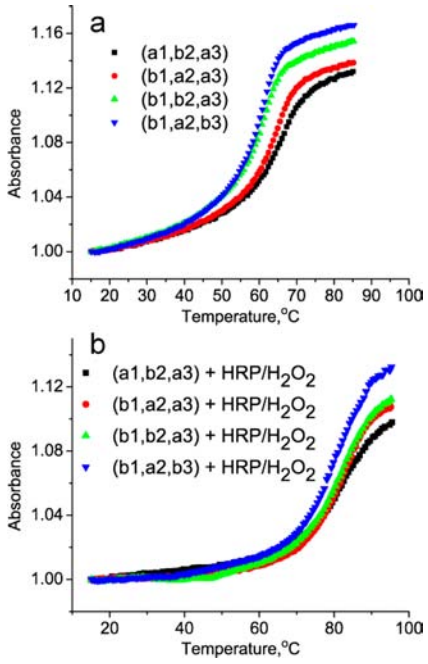

Figure 6. Melting profiles of the cyclic DNA assemblies monitored at 260 nm in buffer solution at pH 4.5: (a) before reaction with HRP/H_2O_2; (b) after reaction with HRP/H_2O_2.

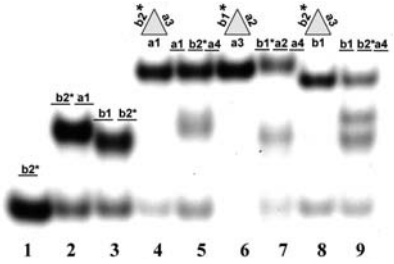

Figure 7. Native PAGE analysis of cyclic and linear modular DNA assemblies. Lane 1, ^{32}P-labeled b2* only; lane 2, (a1,b2*); lane 3, (b1,b2*); lane 4, (a1,b2*,a3); lane 5, (a1,b2*,a4); lane 6, (b1*,a2,a3); lane 7, (b1*,a2,a4); lane 8, (b1,b2*,a3); lane 9, (b1,b2*,a4). The asterisk indicates the radiolabeled strand.

stability of the cyclic assemblies compared with the linear structures observed by T_m is seen in the PAGE as well. The gel for the linear assembly (a1,b2*,a4) shows dimer bands, but formation of the cyclic assembly (a1, b2*,a3) is essentially complete. Similar results are seen for cyclic assembly (b1,b2*,a3) and linear (b1,b2*,a4), lanes 8 and 9, respectively. Because of their cyclic nature, the monomer arrays in assemblies (a1,b2,a3) and in (b1,a2,a3) have the same $(ANi)_5(SNS)_{10}$ pattern, for example. We expect that the isomorphic polymers formed from these structures will have similar properties.

Formation of Cyclic and Linear Copolymers of SNS and ANi. Cyclic Copolymers of SNS and ANi. The results of reaction of cyclic modular assemblies containing SNS and ANi monomers with HRP/H_2O_2 were investigated by means of melting temperature, denaturing PAGE, and UV−vis−NIR spectroscopy. The findings show the formation of cyclic copolymers with programmed sequences of SNS and ANi monomers in high yield.

dx.doi.org/10.1021/ja312507z | J. Am. Chem. Soc. 2013, 135, 4438−4449

Addition of HRP/H_2O_2 to buffer solutions of the cyclic assemblies under mild conditions (5 °C, 10 mM sodium citrate buffer (pH 4.5) containing 200 mM NaCl) results in a dramatic increase in their T_m, see Figure 6b. For example, the product formed from reaction of cyclic assembly (b1,b2,a3) with HRP/H_2O_2 shows a single melting transition with T_m = 82 °C. This corresponds to a ΔT_m of +21.6 °C compared with the unreacted assembly. Similar results are obtained for each of the cyclic assemblies investigated. As a control experiment, we studied the reaction of the single module b2 capped with c3 and c4 (see Figure 5) with HRP/H_2O_2; in this case, no measurable change in T_m is observed.

The reaction of the SNS- and ANi-containing cyclic assemblies with HRP/H_2O_2 initiates oxidative polymerization of the monomers. Bond formation between SNS and ANi monomers will ligate the modules comprising the assembly covalently linking each module by formation of a cyclic copolymer. The melting behavior of the assemblies provides strong evidence for bond formation between all of its monomers. The melting curves observed for the assemblies after reaction with HRP/H_2O_2 shows only one transition, if ligation of the modules was incomplete then two transitions would be observed; one at approximately 60 °C and the second at approximately 80 °C. As shown by the examination of module b2 with caps c3 and c4, polymerization of the monomers without cross-linking does not cause a T_m increase. Finally, the observed ΔT_m of more than 20 °C after reaction with HRP/H_2O_2, corresponding to melting of the duplex arms, shows that cross-linking has made the cyclic assemblies permanent by making the dissociation to separate modules impossible.

The ligated modular assemblies were also analyzed by denaturing PAGE. The results of this analysis for the cyclic assemblies (a1,b2*,a3) and (b1,b2*,a3) are shown in Figure 8.

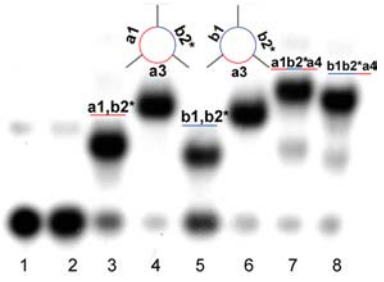

Figure 8. Autoradiography of denaturing PAGE analysis after reaction with HRP/H_2O_2. Lane 1, ^{32}P-labeled b2* only; lane 2, b2*/c3/c4 + HRP/H_2O_2; lane 3, (a1,b2*)/caps + HRP/H_2O_2; lane 4, (a1,b2*,a3) + HRP/H_2O_2; lane 5, (b1,b2*)/caps + HRP/H_2O_2; lane 6, (b1,b2*,a3) + HRP/H_2O_2; lane 7, (a1,b2*,a4)/caps + HRP/H_2O_2; lane 8, (b1,b2*,a4)/caps + HRP/H_2O_2. The asterisk indicates the radiolabeled strand.

Lane 1 shows the positions of modules b2*. Lane 2 shows the results of the reaction of b2* (capped with c3 and c4) with HRP/H_2O_2; it shows that there is no intermolecular cross-linking. Lane 3 shows the results of reaction of b2* and a1 (capped with c1 and c4). Clearly, reaction with HRP/H_2O_2 permanently links modules b2* and a1. The results of reaction of the cyclic assembly (a1,b2*,a3) is shown in lane 4. The denaturing PAGE shows essentially complete ligation of the three modules by formation of the cyclic copolymer with ABA pattern. Similarly, lanes 5 and 6 show the results of the reactions of capped modules (b1,b2*) and cyclic array (b1,b2*,a3), respectively. Again, there is essentially complete ligation of the cyclic array by formation of a cyclic copolymer with a BBA pattern in this case. Interestingly, the copolymer having the BBA pattern migrates slightly faster than that with the ABA pattern. Also shown in Figure 8 are the results of the reaction of linear assemblies with HRP/H_2O_2. Lanes 7 and 8, respectively, show the results for the capped linear arrays (a1,b2*,a4) and (b1,b2*,a4). The former forms a linear copolymer with ABA pattern and the latter has a BBA pattern; these cross-linked assemblies also migrate at different rates. As reported above, the linear assemblies are formed in somewhat lower yield than the cyclic structures.

The optical properties of the cyclic copolymers were assessed by UV−vis−NIR spectroscopy, see Figure 9. Before reaction with HRP/H_2O_2, the cyclic arrays show only absorptions typical of DNA and the SNS monomer (the absorption of the ANi monomer is buried under that of DNA). After reaction with HRP/H_2O_2, the absorptions of the copolymers are characteristic of conducting polymers and are dependent upon the monomer pattern. Figure 9a shows the results for reaction of cyclic assembly (a1,a2,a3), which we have shown previously forms a cyclic homopolymer $(SNS)_{18}$ (an AAA pattern); similarly, Figure 9b is the spectrum of the cyclic homopolymer $(ANi)_{15}$ (a BBB pattern) from reaction of assembly (b1,b2,b3). As expected, these spectra are different. The SNS polymer has a strong band with a peak maximum at approximately 1070 nm, a band at approximately 420, and a weaker band at 540 nm; the ANi polymer has a strong band at approximately 760 nm. The reaction of the assembly formed from modules (b1,a2,a3) with HRP/H_2O_2 forms a cyclic copolymer with the BAA pattern having composition $(ANi)_5(SNS)_{12}$. Its absorption spectrum, Figure 9c, has a strong band at 660 nm that is not observed in the spectra of cyclic $(ANi)_{15}$ or cyclic $(SNS)_{18}$. Significantly, the product formed from reaction of modules (a1,b2,a3) has an absorption spectrum with bands at 420, 660, and 970 nm (Figure 9d) that is essentially identical to that from reaction of modules (b1,a2,a3). This finding is consistent with formation of the DNA-conjoined cyclic $(ANi)_5(SNS)_{12}$ copolymers. In a cyclic array, the ABA and BAA monomer patterns yield identical products. Similar results are observed from the reaction of modules (b1,b2,a3) and (b1,a2,b3), Figure 9f and e, respectively. In these cases, identical cyclic copolymers having the composition $(ANi)_{10}(SNS)_6$ are formed from monomers arrayed in the BBA and BAB pattern. The cyclic $(ANi)_{10}(SNS)_6$ copolymer has a strong absorption band with a maximum at 660 nm and weaker bands at 420, 450, and 960 nm. These results are consistent with those obtained for the linear copolymers prepared by the duplex strategy indicating that the 660 nm absorption band is characteristic of an SNS−ANi copolymer. All of the SNS−ANi copolymers we examined exhibit a characteristic visible absorption at 660 nm and NIR band (960−970 nm). The relative intensity of these two bands is dependent on the ratio of SNS and ANi monomers in the structures. For example, (b1,b2,a3), which forms cyclic $(ANi)_{10}(SNS)_6$, shows a prominent 660 nm band and a weak 950 nm band, while (b1,a2,a3), which forms cyclic $(ANi)_5(SNS)_{12}$, shows a decreased absorption at 660 nm and an increased absorption at 970 nm (see Figure 9). The 10 nm redshift observed in the NIR band for $(ANi)_5(SNS)_{12}$ is consistent with its greater number of SNS monomers. The reduction of these cyclic copolymers with hydrazine results in

dx.doi.org/10.1021/ja312507z | J. Am. Chem. Soc. 2013, 135, 4438−4449

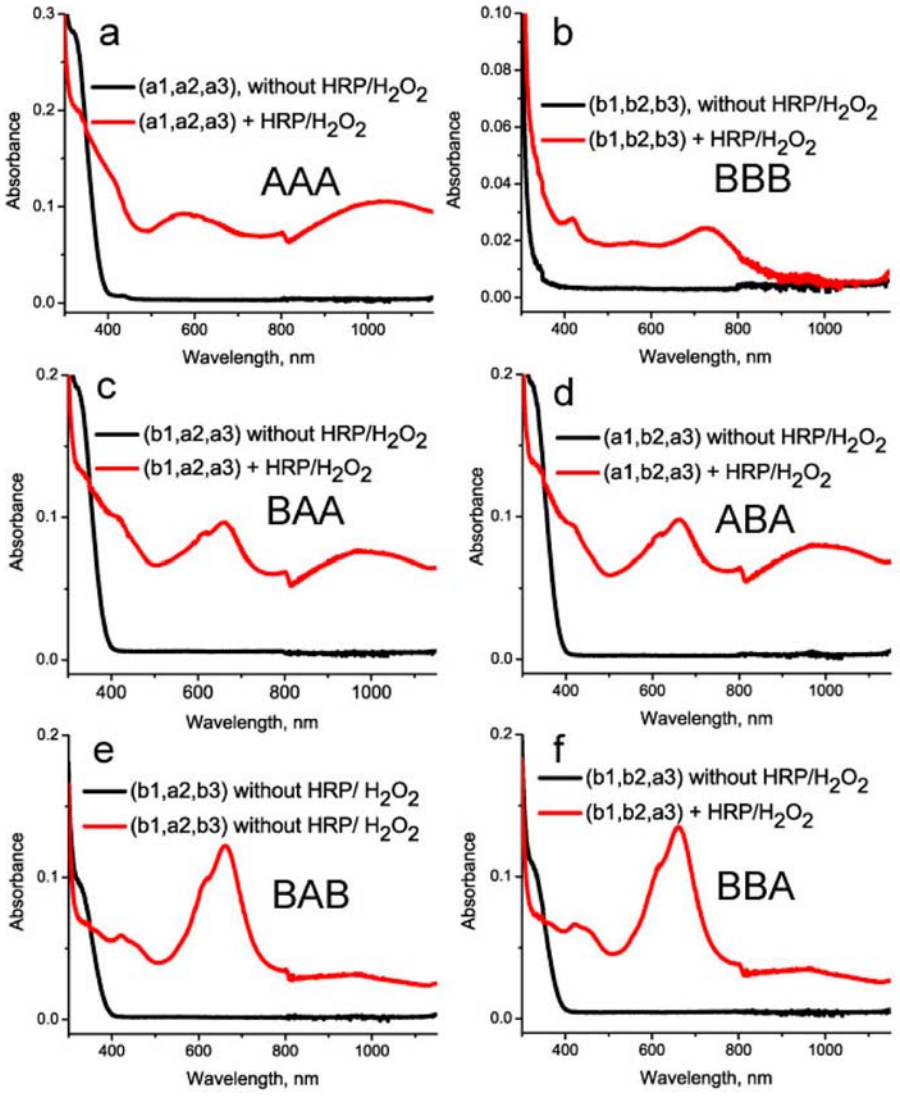

Figure 9. UV−vis−NIR spectra of cyclic DNA assemblies after the reaction with HRP/H_2O_2: (a) (a1,a2,a3); (b) (b1,b2,b3); (c) (b1,a2,a3); (d) (a1,b2,a3); (e) (b1,a2,b3); (f) (b1,b2,a3). The copolymers are identified by their component monomers: A = $(SNS)_6$, and B = $(ANi)_5$. The "glitch" at 800 nm is an instrumental artifact.

the formation of their leuco oxidation states for which the absorption spectra exhibit a shoulder at 400 nm.

The relationship between the vis−NIR polaron/bipolaron bands and the ratio and sequence of SNS and ANi monomers in the copolymers was explored further by examination of four-module assembles, see Scheme 3. Assemblies (b1,a2,a4,a5), (b1,b2,a4,a5), (b1,b2,b4,a5), and (b1,a2,b4,a5) form monomer patterns of BAAA, BBAA, BBBA, and BABA, respectively. These assemblies were shown by melting temperature analysis and by nondenaturing PAGE to be stable cyclic structures (see the Supporting Information, Figure S6−S8 and Table S3).

The UV−vis−NIR spectra of the SNS and ANi copolymers formed from the four-module assemblies by reaction with HRP/H_2O_2 are shown in Figure 10a. The cyclic copolymers that are formed have compositions $(ANi)_5(SNS)_{18}$ from (b1,a2,a4,a5), $(ANi)_{10}(SNS)_{12}$ from (b1,b2,a4,a5), $(ANi)_{15}(SNS)_6$ from (b1,b2,b4,a5), and $(ANi)_5(SNS)_6(ANi)_5(SNS)_6$ from (b1,a2,b4,a5). Figure 10 clearly shows that the intensity of NIR band for SNS−ANi copolymers increases as the number of SNS monomers in the assembly increases; concomitantly, the intensity of the 660 nm band decreases as the number of ANi monomers is reduced. Further, both cyclic assemblies (b1,b2,a4,a5) and (b1,a2,b4,a5) have 12 SNS and 10 ANi monomers, but the former has a

Scheme 3. Illustration of Four-Module DNA-Programmed Cyclic and Linear Assemblies[a]

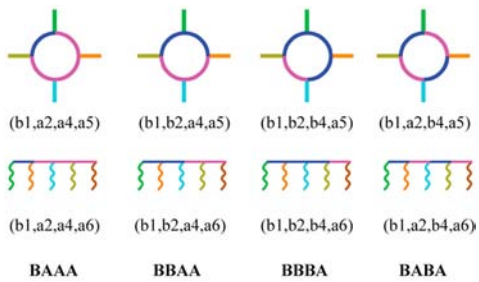

[a]Blue represents ANi-modified segment. Pink represents SNS-modified segment. B represents an $(ANi)_5$ block, and A represents a $(SNS)_6$ block. The structures of the DNA modules are shown in Figure 5.

dx.doi.org/10.1021/ja312507z | J. Am. Chem. Soc. 2013, 135, 4438−4449

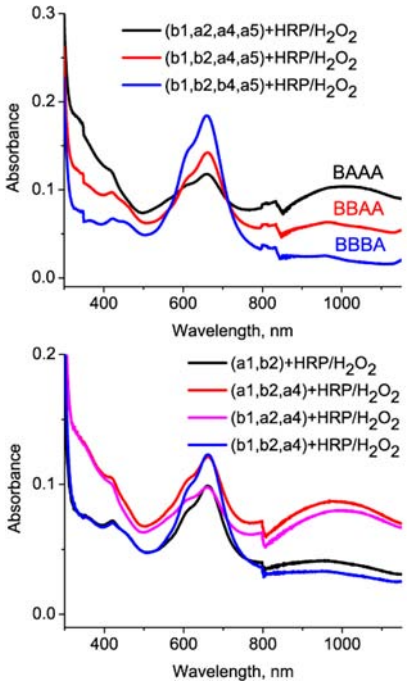

Figure 10. (a) UV−vis−NIR spectra of cyclic DNA assemblies after the reaction with HRP/H_2O_2: (b1,a2,a4,a5); (b1,b2,a4,a5); (b1,b2,b4,a5). (b) UV−vis−NIR spectra of copolymer of SNS and ANi from linear DNA assemblies. The copolymers are identified by their component monomers: A = $(SNS)_6$, and B = $(ANi)_5$. The "glitch" at 800 nm is an instrumental artifact.

BBAA pattern while the latter has a BABA pattern. The UV−vis−NIR spectra recorded after their reaction with HRP/H_2O_2 reflect this difference. The 660 nm band of (b1,a2,b4,a5) is stronger than that of (b1,b2,a4,a5), while the NIR band of (b1,a2,b4,a5) is weaker than that of (b1,b2,a4,a5) (see the Supporting Information, Figure S9). This indicates that bond formation between the monomers of the assemblies is complete and shows that the optical properties of the cyclic copolymers of SNS and ANi can be tuned by changing the monomer ratio and also by controlling the specific sequence of monomers in the assembly.

The composition of the cyclic copolymers can also be controlled by varying the number of monomers linked to each module. For example, an encoded module bearing 10 ANi monomers forms the cyclic three-module copolymer $(ANi)_{10}(SNS)_{12}$ that is identical with that from the four-module assembly (b1,b2,a4,a5) that also forms the cyclic $(ANi)_{10}(SNS)_{12}$ copolymer. Similarly, three- and four-module cyclic assemblies both produce the identical $(ANi)_{15}(SNS)_6$ copolymer (see the Supporting Information, Figure S10).

Linear Copolymers of SNS and ANi. The addition of HRP/H_2O_2 to linear modular assemblies (b1,a2,a4), (a1,b2,a4), and (b1,b2,a4) with their terminal single strands capped by c1 and c2, see Scheme 2, yields linear copolymers with patterns BAA, ABA, and BBA, respectively. The products of these reactions were investigated by melting temperature, denaturing PAGE, and by UV−vis−NIR spectroscopy. After reaction with HRP/H_2O_2, the melting curve for assembly (b1,b2,a4) with caps c1 and c2 has two transitions: the first appears at approximately 45 °C and corresponds to denaturation of the capping oligomers, and the second occurs at approximately 80 °C, which corresponds to melting of the "arms" of the ligated cross-linked modules (see the Supporting Information, Figure S12 and Table S2). The formation of linear copolymers was confirmed by denaturing PAGE. Figure 8 lanes 7 and 8 show the efficient formation of linear copolymers from modules (a1,b2,a4) and (b1,b2,a4) corresponding to linear ABA and BBA patterns, respectively. The absorption spectra of these copolymers, Figure 10b, show bands with maxima at 660 nm and at approximately 960 nm that are characteristic of the oxidized copolymers. The relative intensities of these bands reflect the structural uniqueness of the copolymers. In general, the relative intensity of the NIR band increases with the number of SNS monomers. Significantly, in contrast to the cyclic assemblies where the BAA and ABA patterns give identical copolymers, in the linear assemblies (b1,a2,a4) and (a1,b2,a4), the BAA and ABA patterns give different copolymers having different optical properties; the linear ABA copolymer has a stronger absorption at 660 nm than the linear BAA copolymer.

DISCUSSION

One of the principal goals of synthetic polymer chemistry is to develop methods to construct sequence-controlled polymers similar to those observed in natural macromolecules such as proteins and nucleic acids.[1] Many routes have been explored for this purpose, but among these efforts, DNA-templated polymerization is noteworthy because of the unique sequence-recognizing and self-organizing properties of DNA.[7−13] Developments in DNA-based structural nanotechnology have enabled its use as a building block to make various regular and irregular one-, two-, and three-dimensional nanostructures.[35−37] Polymers made on such DNA templates can have controlled structures that are defined by the sequence of nucleobases. As a demonstration of this concept, we previously reported the preparation of cyclic and linear SNS polymers conjoined to modular DNA assemblies.[27] Here, we have demonstrated the formation of SNS and ANi copolymers on DNA scaffolds that highlight the facile sequence programmability made possible by this approach. Copolymerization of a pair of monomers leads to an increase in the number of conducting polymers that can be made from the same set of monomers. Moreover, it is certain that these copolymers will have unique chemical and physical properties.

Bond Formation between SNS and ANi Monomers in DNA-Conjoined Copolymers. Conducting polymers such as polyaniline, polythiophene, and polypyrrole have received considerable attention because of their remarkable electronic, magnetic, and optical properties.[38,39] Most studies of conducting polymers have focused on homopolymers that are prepared either through the chemical or electrochemical polymerization of a single monomer type. A few studies have described the synthesis of conducting copolymers from aniline and pyrrole[40−42] or thiophene.[43−46] Previously, copolymers of aniline and pyrrole or thiophene have been characterized by means of X-ray photoelectron spectroscopy, Fourier transform IR spectroscopy, UV−vis spectroscopy, and cyclic voltammetry, which demonstrated that they were not the mixtures of two homopolymers; however, there was no conclusive proof of bond formation between aniline and thiophene or pyrrole monomers.[47] The DNA-programmed assembly process reported here provides proof for ANi to SNS bond formation.

Bond formation between SNS and ANi monomers in the duplex strategy cross-links SNS- and ANi-containing oligomers, and in the encoded module strategy, bond formation ligates

dx.doi.org/10.1021/ja312507z | J. Am. Chem. Soc. 2013, 135, 4438−4449

two DNA oligomers. The results reported above for both strategies clearly demonstrate that the reaction of these assemblies with HRP/H_2O_2 causes bond formation between ANi and SNS monomers and the formation of linear and cyclic $(SNS)_n(ANi)_m$ block copolymers of defined sequence and composition. The most direct evidence for bond formation between ANi and SNS monomers comes from denaturing PAGE analysis of the reaction products, which reveals the formation of cross-linked or ligated DNA oligomers in high yield. Evidently, when the ANi and SNS monomers are held in a fixed arrangement in close proximity, bond formation between them is very efficient.

Bond formation between the DNA-linked ANi and SNS monomers can occur in a head-to-head or head-to-tail orientation. In the presence of a template, ANi monomers are prone to react in a head–tail manner forming a conjugated polymer.[18−21] In previous work on the DNA-directed synthesis of conducting polymers, we demonstrated a preference for head-to-tail coupling of ANi and of SNS monomers in the homopolymers.[23,25,26] In the case of the copolymers of aniline and thiophene, others have concluded that bond formation in the polymerization of 4-(2-thienyl)benzenamine initiated by $FeCl_3$ occurs at the benzenamine group and the free α-position of thiophene moiety.[48] The UV–vis–NIR spectra of the ANi and SNS copolymers described above show typical absorption features of $(ANi)_n$ and $(SNS)_m$ in the head-to-tail configuration. These findings suggest that the overall structure of ANi and SNS copolymers described here have the conjugated head-to-tail orientation (see the Supporting Information, Figure S14).

Figure 11 shows geometry optimized schematic structures for the linear DNA-conjoined head-to-tail copolymer formed from

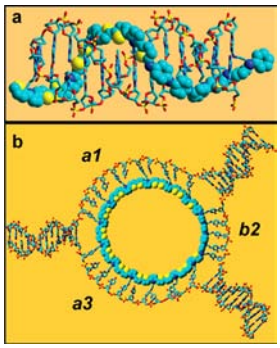

Figure 11. Three-dimensional geometry optimized structures of copolymers: (a) $(SNS)_4(ANi)_6$ on DNA(1,2); (b) cylic $(ANi)_5(SNS)_{12}$ on (a1,b2,a3). The copolymers are highlighted by colored sphere structures: cyan, carbon; blue, nitrogen; yellow, sulfur. The structures are obtained using HyperChem 8.5.

duplex DNA(1,2) and for the cyclic copolymer formed from modules (a1,b2,a3).[25,26] In the linear structure, Figure 11a, the $(SNS)_4(ANi)_6$ copolymer appears as a third strand that occupies the major groove of canonical duplex DNA. Consistent with the observed CD spectra, see Figure 2, the DNA scaffold maintains a B-form-like structure. The cyclic, three-arm structure, Figure 11b, shows the $(ANi)_5(SNS)_{12}$ copolymer as a ring linked to the DNA scaffold. Both structures suggest the great flexibility inherent in the DNA-programmed approach to the assembly of these copolymers. Not only can the overall structural form (linear or cyclic) be easily created, but the method of construction provides opportunities for simple manipulation of the length and the specific composition of these copolymers.

Sequence Control of DNA-Conjoined SNS and ANi Copolymers. The construction of SNS and ANi copolymers with building blocks composed of monomers covalently linked to a nucleobase (e.g., cytosine) enables the use of convenient machine-based synthesis to prepare DNA oligomers bearing these monomers in an organized and predesigned pattern or sequence. The reaction of these preorganized monomers with HRP/H_2O_2 leads efficiently to unique copolymers. This approach was demonstrated successfully by the copolymerization of SNS and ANi monomers employing the duplex strategy to form programmed linear arrays from monomers on complementary strands and by means of the encoded modules strategy to form linear and cyclic copolymers. The DNA-conjoined copolymers $(SNS)_4(ANi)_6$ and $(ANi)_2(SNS)_2(ANi)_2(SNS)_2(ANi)_2$ were conveniently prepared using the duplex strategy. This approach is satisfactory for preparing linear copolymers. However, its applicability is limited to short copolymers because the stability of the duplex decreases as the number of covalently linked monomers increases.

The encoded module strategy enables the facile preparation of cyclic and linear copolymers of ANi and SNS of variable length and of designed sequence. A significant advantage of this approach is that the stability of DNA assembly is not deteriorated by the presence of the SNS or ANi monomers because the modified segments do not participate in the Watson–Crick association. In fact, we observe that the formation of SNS and ANi cyclic arrays actually stabilize the modular assembly through hydrophobic interactions between the monomers.[34] Significantly, the encoded module strategy allows for easy control of the sequence of SNS and ANi monomers simply by hybridizing appropriately modified modules.

As outlined in Schemes 2 and 3, assemblies of SNS and ANi monomers in cyclic or linear arrays are readily prepared by the programmed assembly of encoded modules. For example, cyclic and linear copolymers with BAA, ABA, BBA, and BAB patterns are obtained from the reaction of modular arrays (b1,a2,a3/4), (a1,b2,a3/4), (b1,b2,a3/4), and (b1,a2,b3/4) with HRP/H_2O_2. The different sequences of SNS and ANi monomers in the copolymers are reflected by their unique UV–vis–NIR spectra. The ability to define the sequence of SNS and ANi monomers in the copolymers formed by modular assembly was demonstrated both by selecting the modules for assembly and by adjusting the number of monomers linked to a module. For example, cyclic copolymers having the sequences $(SNS)_{12}(ANi)_{10}$ and $(SNS)_{12}(ANi)_5$ were prepared simply by changing the number of ANi monomers in the central segment of a module. To demonstrate the flexibility of the encoded module strategy, the cyclic copolymer $(SNS)_{12}(ANi)_{10}$ was also prepared by reaction of the four module assembly (b1,b2,a4,a5). As expected, the properties of the copolymer are independent of the way in which it is prepared.

Optical Properties of SNS and ANi Copolymers. The unique optical properties of the DNA-conjoined copolymers of SNS and ANi reflect their unique structures. The UV–vis–NIR spectra of the copolymers are obviously different from those of the homopolymers. The copolymers show spectral features of both homopolymers in their oxidized states.[21,26,27,49] The blueshift of the benzenoid–quinoid exciton transition band, 660 nm for copolymer and 730 nm for polyaniline, reflects the

dx.doi.org/10.1021/ja312507z | J. Am. Chem. Soc. 2013, 135, 4438−4449

change caused by covalent linkage between $(SNS)_m$ and $(ANi)_n$ blocks. The unique absorption spectra of copolymer of SNS and ANi combined with the demonstration of bond formation between SNS and ANi indicate that SNS and ANi segments are linked in a head-to-tail manner.

The optical spectra of the SNS and ANi copolymers are dependent on the ratio and order of monomers. The DNA modular assembly strategy enables the precise control of the number of SNS and ANi monomers comprising the copolymer. For example, in the four-arm cyclic assemblies, see Scheme 3, the ratio of SNS and ANi in the copolymer was systematically changed from $(SNS)_{18}(ANi)_5$ to $(SNS)_{12}(ANi)_{10}$ and $(SNS)_6(ANi)_{15}$.The intensity of the NIR absorption band for these polymers decreases regularly as the number of SNS monomers in the copolymer decreases; concomitantly, the intensity of the 660 nm band increases with the number of ANi monomers. This clearly demonstrates the optical properties of the copolymer are tunable in a precise tailor-made fashion by the DNA modular self-assembly strategy. It is likely that all physical properties of the copolymers will depend uniquely on their composition.

CONCLUSIONS

Cyclic and linear DNA-conjoined copolymers of SNS and ANi have been synthesized by the duplex and encoded modular self-assembly strategies. Facile, precise sequence control of SNS and ANi monomers has been achieved. The hybridization of DNA oligomers containing covalently linked SNS and ANi monomers creates ordered linear and cyclic arrays with specific monomer sequences. The reaction of these monomer arrays with HRP/H_2O_2 forms copolymers in high yield, demonstrating bond formation between SNS and ANi monomers. The unique properties of the copolymers of SNS and ANi in various oxidation states are revealed by UV−vis−NIR spectroscopic measurements. The correlation between the optical spectra and monomer sequences of these copolymers suggests that other properties such as electric conduction and magnetic susceptibility of these materials will also be specifically controllable. It is interesting to point out that these DNA-conjoined copolymers are nanowires with specific length and defined structure. With the development of DNA nanotechnology, we anticipate that these new materials may be built into super arrays and find application in microelectronic devices and nanosensors.

ASSOCIATED CONTENT

Supporting Information

Mass analysis of SNS−DNA and ANi−DNA oligomers; melting profiles of DNA(1,2) and DNA(3,4) before and after reaction with HRP/H_2O_2; UV−vis spectra of DNA (1,2) and DNA(3,4); UV−vis spectra of DNA(1,2) and DNA(3,4) after the reaction with HRP/H_2O_2 and reduction with hydrazine; melting profiles of linear DNA assemblies; T_m of cyclic and linear assemblies before and after reaction with HRP/H_2O_2; melting profiles of four-module cyclic DNA assemblies; T_m of cyclic DNA assemblies before and after reaction with HRP/H_2O_2; native PAGE analysis of four-module cyclic DNA assemblies; denaturing PAGE analysis of the modular DNA assemblies after the reaction with HRP/H_2O_2; UV−vis−NIR spectra of (b1,b2,a4,a5) and (b1,a2,b4,a5) with the addition of HRP/H_2O_2; UV−vis−NIR spectra of cyclic DNA assemblies after the reaction with HRP/H_2O_2. Denaturing PAGE analysis of modular DNA assemblies after the reaction with HRP/H_2O_2; head-to-tail structure of copolymer of SNS and ANi; and three-dimensional geometry optimized structures of copolymers. This material is available free of charge via the Internet at http://pubs.acs.org.

AUTHOR INFORMATION

Corresponding Author

Schuster@gatech.edu

Notes

The authors declare no competing financial interest.

ACKNOWLEDGMENTS

This work is supported by the Vasser Woolley Foundation, for which we are grateful.

REFERENCES

(1) Badi, N.; Lutz, J. F. *Chem. Soc. Rev.* **2009**, *38*, 3383.
(2) Shen, J. Z.; Sogah, D. Y. *Macromolecules* **1994**, *27*, 6996.
(3) Kramer, J. W.; Treitler, D. S.; Dunn, E. W.; Castro, P. M.; Roisnel, T.; Thomas, C. M.; Coates, G. W. *J. Am. Chem. Soc.* **2009**, *131*, 16042.
(4) Ida, S.; Terashima, T.; Ouchi, M.; Sawamoto, M. *J. Am. Chem. Soc.* **2009**, *131*, 10808.
(5) Ouchi, M.; Badi, N.; Lutz, J.-F.; Sawamoto, M. *Nat. Chem.* **2011**, *3*, 917.
(6) Nakatani, K.; Ogura, Y.; Koda, Y.; Terashima, T.; Sawamoto, M. *J. Am. Chem. Soc.* **2012**, *134*, 4373.
(7) McHale, R.; O'Reilly, R. K. *Macromolecules* **2012**, *45*, 7665.
(8) Orgel, L. E. *Acc. Chem. Res.* **1995**, *28*, 109.
(9) Li, X.; Zhan, Z.-Y. J.; Knipe, R.; Lynn, D. G. *J. Am. Chem. Soc.* **2002**, *124*, 746.
(10) Rosenbaum, D. M.; Liu, D. R. *J. Am. Chem. Soc.* **2003**, *125*, 13924.
(11) Kleiner, R. E.; Brudno, Y.; Birnbaum, M. E.; Liu, D. R. *J. Am. Chem. Soc.* **2008**, *130*, 4646.
(12) Schrum, J. P.; Ricardo, A.; Krishnamurthy, M.; Blain, J. C.; Szostak, J. W. *J. Am. Chem. Soc.* **2009**, *131*, 14560.
(13) Ravnsbæk, J. B.; Jacobsen, M. F.; Rosen, C. B.; Voigt, N. V.; Gothelf, K. V. *Angew. Chem., Int. Ed.* **2011**, *50*, 10851.
(14) Hassanien, R.; Al-Hinai, M.; Farha Al-Said, S. A.; Little, R.; Šiller, L.; Wright, N. G.; Houlton, A.; Horrocks, B. R. *ACS Nano* **2010**, *4*, 2149.
(15) Tang, H. W.; Chen, L. L.; Xing, C. F.; Guo, Y. G.; Wang, S. *Macromol. Rapid Commun.* **2010**, *31*, 1892.
(16) Bruno, F. F.; Fossey, S. A.; Nagarajan, S.; Nagarajan, R.; Kumar, J.; Samuelson, L. A. *Biomacromolecules* **2005**, *7*, 586.
(17) Nagarajan, S.; Kumar, J.; Bruno, F. F.; Samuelson, L. A.; Nagarajan, R. *Macromolecules* **2008**, *41*, 3049.
(18) Nagarajan, R.; Liu, W.; Kumar, J.; Tripathy, S. K.; Bruno, F. F.; Samuelson, L. A. *Macromolecules* **2001**, *34*, 3921.
(19) Liu, W.; Kumar, J.; Tripathy, S.; Senecal, K. J.; Samuelson, L. *J. Am. Chem. Soc.* **1998**, *121*, 71.
(20) Liu, W.; Cholli, A. L.; Nagarajan, R.; Kumar, J.; Tripathy, S.; Bruno, F. F.; Samuelson, L. *J. Am. Chem. Soc.* **1999**, *121*, 11345.
(21) Nagarajan, R.; Tripathy, S.; Kumar, J.; Bruno, F. F.; Samuelson, L. *Macromolecules* **2000**, *33*, 9542.
(22) Chen, W.; Josowicz, M.; Datta, B.; Schuster, G. B.; Janata, J. *Electrochem. Solid-State Lett.* **2008**, *11*, E11.
(23) Datta, B.; Schuster, G. B. *J. Am. Chem. Soc.* **2008**, *130*, 2965.
(24) Srinivasan, S.; Schuster, G. B. *Org. Lett.* **2008**, *10*, 3657.
(25) Datta, B.; Schuster, G. B.; McCook, A.; Harvey, S. C.; Zakrzewska, K. *J. Am. Chem. Soc.* **2006**, *128*, 14428.
(26) Chen, W.; Guler, G.; Kuruvilla, E.; Schuster, G. B.; Chiu, H. C.; Riedo, E. *Macromolecules* **2010**, *43*, 4032.
(27) Chen, W.; Schuster, G. B. *J. Am. Chem. Soc.* **2012**, *134*, 840.
(28) Nguyen, T.; Brewer, A.; Stulz, E. *Angew. Chem., Int. Ed.* **2009**, *48*, 1974.

(29) Chen, W.; Schuster, G. B. *Org. Biomol. Chem.* **2013**, *11*, 35.
(30) Asanuma, H.; Shirasuka, K.; Takarada, T.; Kashida, H.; Komiyama, M. *J. Am. Chem. Soc.* **2003**, *125*, 2217.
(31) Jung, J.-A.; Lee, S. H.; Jin, B.; Sohn, Y.; Kim, S. K. *J. Phys. Chem. B* **2010**, *114*, 7641.
(32) Song, H. K.; Palmore, G. T. R. *Adv. Mater.* **2006**, *18*, 1764.
(33) Song, H.-K.; Palmore, G. T. R. *J. Phys. Chem. B* **2005**, *109*, 19278.
(34) Ma, Z.; Chen, W.; Schuster, G. B. *Chem. Mater.* **2012**, *24*, 3916.
(35) Ke, Y.; Ong, L. L.; Shih, W. M.; Yin, P. *Science* **2012**, *338*, 1177.
(36) Wei, B.; Dai, M.; Yin, P. *Nature* **2012**, *485*, 623.
(37) Seeman, N. C. *Annu. Rev. Biochem.* **2010**, *79*, 65.
(38) Pecher, J.; Mecking, S. *Chem. Rev.* **2010**, *110*, 6260.
(39) Park, D. H.; Kim, M. S.; Joo, J. *Chem. Soc. Rev.* **2010**, *39*, 2439.
(40) Xu, P.; Han, X. J.; Wang, C.; Zhang, B.; Wang, H. L. *Synth. Met.* **2009**, *159*, 430.
(41) Wen, T. C.; Yang, C. H.; Chen, Y. C.; Lin, W. C. *J. Electrochem. Soc.* **2003**, *150*, D123.
(42) Antony, M. J.; Jayakannan, M. *J. Phys. Chem. B* **2011**, *115*, 6427.
(43) Liang, Q. Y.; Neoh, K. G.; Kang, E. T.; Tan, K. L.; Wong, H. K. *Eur. Polym. J.* **1992**, *28*, 755.
(44) Udum, Y. A.; Pekmez, K.; Yıldız, A. *Eur. Polym. J.* **2005**, *41*, 1136.
(45) Özçiçek, N. P.; Pekmez, K.; Holze, R.; Yıldız, A. *J. Appl. Polym. Sci.* **2003**, *90*, 3417.
(46) Dufour, B.; Rannou, P.; Travers, J. P.; Pron, A.; Zagórska, M.; Korc, G.; Kulszewicz-Bajer, I.; Quillard, S.; Lefrant, S. *Macromolecules* **2002**, *35*, 6112.
(47) Holze, R. *Electrochim. Acta* **2011**, *56*, 10479.
(48) Ng, S.-C.; Xu, L. *Adv. Mater.* **1998**, *10*, 1525.
(49) Malinauskas, A.; Holze, R. *Synth. Met.* **1998**, *97*, 31.